p wave, the Born approximation yields the same phase shifts as those obtained from a Schrödinger analysis.

We have just noted the substantial agreement between the Born approximation and Schrödinger theory for the case of van der Waals scattering. The fact that the Born approximation works so well for

long-range forces has been discussed in previous articles.[7,8] Basically, the long-range forces give additional contributions precisely because of their long-range character; but at long ranges the potentials are arbitrarily weak, and therefore the leading terms are obtained exactly in the Born approximation, just as found above.

[1]M. H. Mittleman and K. M. Watson, Phys. Rev. 113, 198 (1959); M. H. Mittleman, Ann. Phys. (N.Y.) 14, 94 (1961); A. Dalgarno, Advan. Phys. 11, 281 (1962); C. J. Kleinman, Y. Hahn, and L. Spruch, Phys. Rev. 165, 53 (1968); A. Dalgarno, G. W. F. Drake, and G. A. Victor, ibid. 176, 194 (1968).

[2]O. Hinckelmann and L. Spruch, Phys. Rev. A 3, 642 (1971).

[3]I. S. Gradshteyn and I. M. Ryzhik, Tables of Integrals, Series and Products (Academic, New York, 1965).

[4]G. N. Watson, Theory of Bessel Functions (Cambridge U.P., London, 1966).

[5]Handbook of Mathematical Functions, edited by M. Abramowitz and I. A. Stegun (Dover, New York, 1965).

[6]P. S. Ganas, Phys. Rev. A 4, 2224 (1971).

[7]L. Spruch, T. F. O'Malley, and L. Rosenberg, Phys. Rev. Letters 5, 375 (1960).

[8]T. F. O'Malley, L. Spruch, and L. Rosenberg, J. Math. Phys. 2, 491 (1961).

Ionization of K Atoms in Collision with H₂, N₂, O₂, and CO[†]

J. F. Cuderman

Sandia Laboratories, Albuquerque, New Mexico 87115

(Received 1 November 1971)

Absolute cross sections are reported here for the ionization of K atoms having laboratory energies in the range 20–1000 eV when interacting with H_2, N_2, O_2, and CO molecules. The range of energies covered, E, and the corresponding cross sections σ_{01} for each of the four target species are as follows: for O_2, $20 < E < 1000$ eV, $8 \times 10^{-19} < \sigma_{01} < 1.1 \times 10^{-15}$ cm²; for N_2, $50 < E < 1000$ eV, $2.5 \times 10^{-19} < \sigma_{01} < 4 \times 10^{-17}$ cm²; for CO, $100 < E < 1000$ eV, $2 \times 10^{-19} < \sigma_{01} < 2.3 \times 10^{-17}$ cm²; for H_2, $150 < E < 1000$ eV, $6 \times 10^{-20} < \sigma_{01} < 8 \times 10^{-18}$ cm².

I. INTRODUCTION

This paper describes the measurement of the absolute cross sections for ionization of K atoms on impact with diatomic atmospheric constituents. The cross sections are presented as a function of K-atom velocity from near threshold for the reaction to 1000 eV. From conservation of energy and momentum considerations, the threshold energy E_0 in the laboratory system for the ionization process is

$$E_i = M_1 E_0/(M_1 + M_2) , \tag{1}$$

where E_i is the amount of energy required to ionize potassium (4.3 eV) and M_1 and M_2 are the respective masses of the target molecules and potassium projectile atoms.

There are a number of reasons for choosing the alkali metals for the projectile atoms. The alkali-metal atoms are, in the first approximation, hydrogenic and therefore perhaps more amenable to analysis than other species. The fact that they are condensible made it possible to build a charge-transfer-type fast-atom accelerator which has little

or no slow-atom contamination in the beam. The alkali-metal atoms have large resonant charge-transfer cross sections, and they can be detected using surface ionization techniques. The choice of potassium for the initial measurements is appropriate because to date it is the only alkali-metal atom whose surface ionization behavior has been investigated as a function of energy for the range 0–1000 eV.[1-3] There exist a number of recent measurements of low-energy ionization cross sections involving neutral targets and projectiles in the range from threshold to a few hundred eV.[4-14] However, very few of these include alkali-metal atoms. In particular, for the ionization reactions considered here, no previous data appear to exist below 150 eV. For H_2, N_2, and O_2 comparison is possible with the data of Bydin and Bukhteev[14] which span the range from 150–2200 eV. In addition there are the higher-energy data of Kikiani et al.[15] which go from 3 to 15 keV.

II. EXPERIMENTAL APPARATUS

A. Vacuum System

Figure 1 is a schematic of the over-all experi-
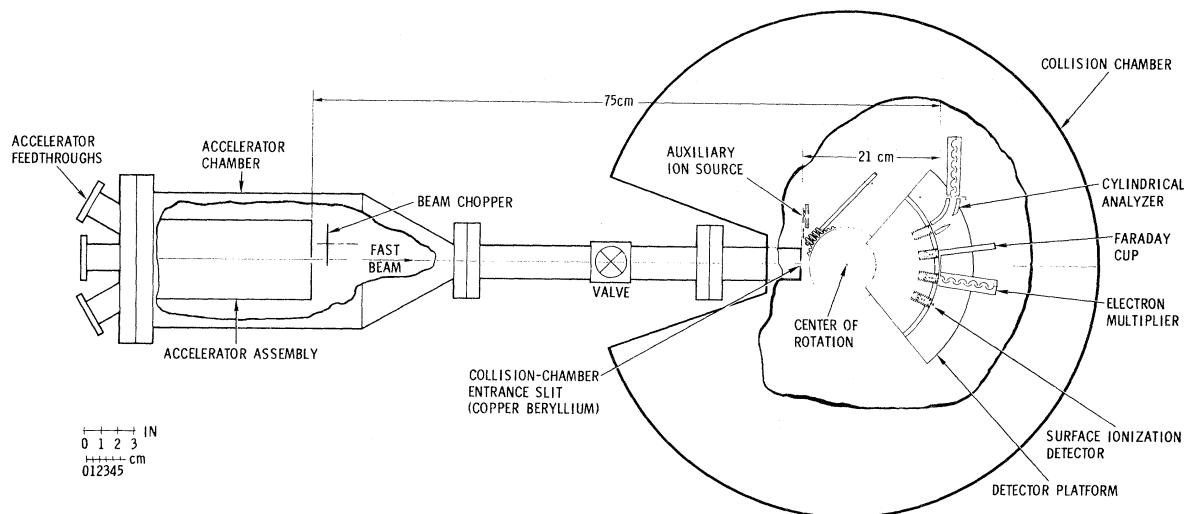
NOTE: ALL VACUUM CHAMBER
ASSEMBLIES 304SS

FIG. 1. Experimental schematic.

mental setup. It consists of the fast-atom accelerator, and a collision chamber which contains the detection apparatus. The two systems are connected through a straight-through valve which permits isolation of either system. In addition, just before entering the collision chamber, the fast-atom beam undergoes final collimation by a vertical slit 1.27 mm wide by 10 mm long. This slit also serves to permit the accelerator chamber to be differentially pumped relative to the collision chamber. Both chambers are evacuated by 6-in. mercury diffusion pumps. Typical background pressures are 1×10^{-8} Torr in both chambers. During experimental measurements when the collision chamber is backfilled to 1×10^{-5} Torr of target gas, the accelerator chamber pressure does not exceed 1×10^{-7} Torr.

B. Accelerator

The fast-atom accelerator is of the resonant charge-transfer type. K ions are obtained from a thermionic zeolite source. These ions are accelerated to a selected energy between 5 and 1000 eV and then resonantly charge exchanged by interaction with a crossed beam of K atoms emitted from an effusion oven operated at 300 °C. The resulting fast-beam flux is typically 10^{8}–10^{10} sec^{-1} corresponding, respectively, to the lower and upper energy limits of the accelerator. The entire accelerator assembly is enclosed in a liquid-nitrogen-cooled manifold to reduce thermal-K-atom background in the fast beam. The success of the design is such that when the fast-beam flux at the exit aperture of the accelerator is 10^{8} to 10^{10} sec^{-1}, the thermal-atom flux, measured when the ion source is turned off, is less than 10^{4} sec^{-1}.

Figure 2 schematically shows the important design features of the accelerator including parts of the assembly which are directly cooled by flowing liquid nitrogen through them. As is shown, the accelerator consists of the ion source, extraction lens system, two double-aperture lenses, an einsel lens, charge-transfer region, deflection plates, and beam chopper.

The ion source consists of a small bead of potassium zeolite about 3 mm in diameter and 0.5 mm thick which is fused onto a strip of Pt mesh whose dimensions are approximately 3 mm by 20 mm. The source is heated to approximately 1000 °C by passing about 10 A of dc current through it. The procedure for fabricating the source was first described by Weber and Cordes.[16]

The extractor lens system forms the ions from the source into a beam and accelerates them to about 200 eV. The voltages used for the extraction lenses are shown. The two double aperture lenses essentially determine the fast-beam energy, although the exit aperture of the second lens may still be a few volts below that of the entrance aperture of the einsel lens. The double aperture lens voltage ratios are about 3 and 2.4, respectively, as shown in Fig. 2.

The einsel lens assembly then focuses the resulting beam into the charge-transfer region for maximum fast neutral flux at the target. The outer apertures of the einsel lens are held, together with the charge transfer region, at the same potential as the desired fast-beam energy. The inner aperture of the einsel lens is varied to produce the desired focus.

The charge-transfer region consists of a slotted

NOTE: 1. ALL METAL DETAILS FABRICATED
OF TYPE 304 STAINLESS STEEL
EXCEPT AS NOTED

2. ALL INSULATOR SPACERS AND
STAND OFF FABRICATED OF Al_2O_3

FAST BEAM

BEAM CHOPPER

ACCELERATOR EXIT
APERTURE
(COPPER BERYLLIUM)

DEFLECTION
PLATES

$-300V$ $+200V$

LIQ. N_2 PASSAGE

LIQ. N_2 OUT

LIQ. N_2 IN

CHARGE-TRANSFER
CYLINDER

CRINKLY-FOIL
EMITTER
(0.0005-THICK
IRON)

CHARGE-
TRANSFER
OVEN
(ARMCO
IRON)

GLASS CAPSULE
ENCASED IN
STEEL WOOL

EINSEL
LENSE

VARIABLE FOR
BEST FOCUS

$\sim 2.4V_2$

SECOND
DOUBLE-
APERTURE
LENSE

V_2

LIQUID N_2 CHANNEL

CERAMIC SUPPORT ROD

CERAMIC SPACER

$-200V$
$-125V$
$-250V$

$\sim 3V_1$

FIRST DOUBLE-
APERTURE LENSE

V_1

ENTRACTOR
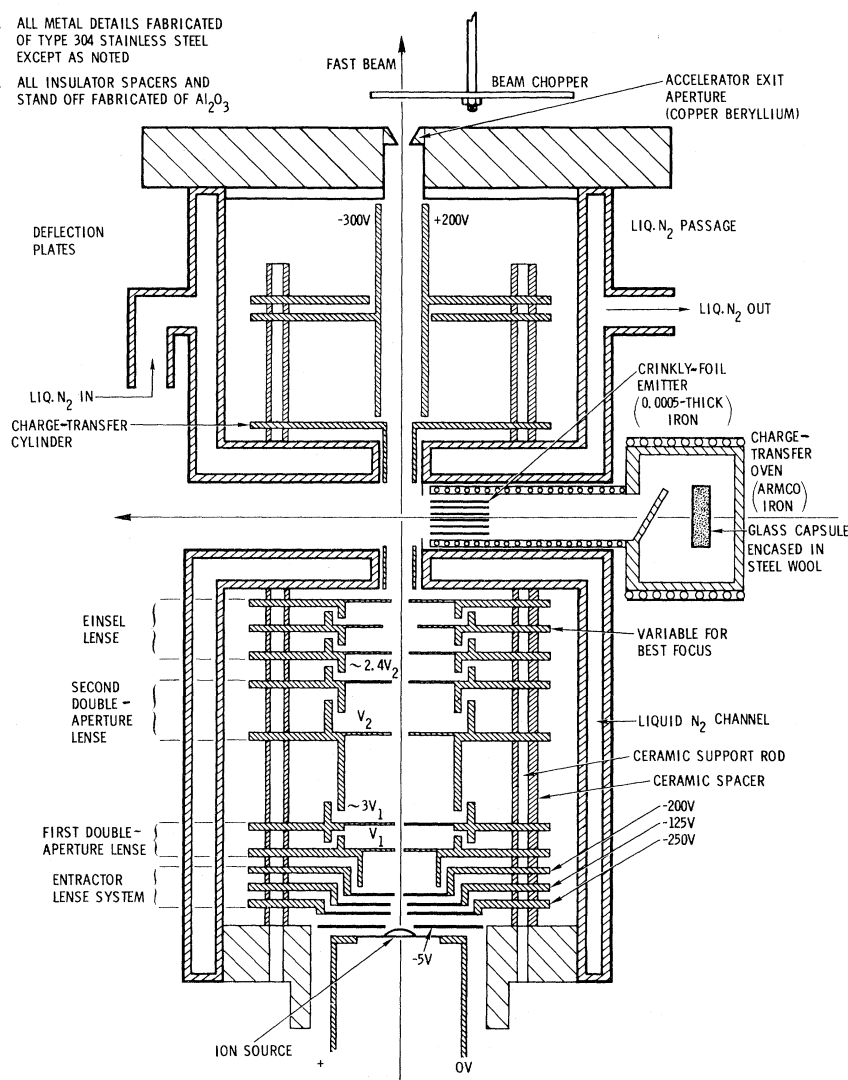LENSE SYSTEM

$-5V$

ION SOURCE

$+$ $0V$

FIG. 2. Accelerator
schematic.

cylinder through which the beam from the effusion oven passes. Chilled surfaces surround the charge-transfer cylinder and precollimate the beam to minimize deposition of potassium on the cylinder.

The thermal effusion oven is of the crinkly-foil type[17] and consists of two chambers. The first chamber is the reservoir in which a capsule of potassium is placed and packed in a small wad of steel wool. The second chamber is connected to the reservoir and contains the crinkly-foil effuser. The reservoir is typically operated at 295–300 °C and the effuser chamber at about 400 °C.

Finally, the beam chopper performs a number of functions during data-taking operations. We have used it during calibration of surface ionization detectors for fast-atom detection where phase-sensitive detection was required, as an on-off beam flag, and to overcome electrometer drift by modulating the fast beam and measuring the amount of offset

in output on a strip chart recorder superimposed on drift during "on times."

C. Detection System

Figure 1 also schematically shows the detection system. It consists of an electron multiplier, Faraday cup, cylindrical analyzer with attached electron multiplier, and a surface ionization detector. Each detector is preceded by twin collimating apertures of 3.18-mm diameter which are 2.54 cm apart. The collimating apertures are all fabricated of copper beryllium which has a low work function and which therefore eliminates the possibility of "cold surface ionization" of fast-beam particles at the apertures. The detectors are mounted on a precision machined platform which rotates about the center of rotation indicated and is externally actuated. A movable externally actuated auxiliary ion source is mounted to one side of the entrance

slit to the collision chamber. This source can be moved in front of the entrance slit to provide an ion beam which intersects the detector rotation axis. This ion beam is used to calibrate the ion detectors. The auxiliary ion source consists of an einsel lens preceded by a K zeolite ion source.

The electron multiplier monitors the fast-K-atom profile and, in particular, monitors the fast-beam flux during adjustment of the accelerator focus for maximum intensity. Its effectiveness for this purpose has been previously described. [18]

The Faraday cup is an absolute detector which permits calibration of the cylindrical analyzer-electron multiplier combination.

The cylindrical analyzer is a 63. 5° instrument. The analyzer separates the K ions produced in collisions with gas-target atoms from the accompanying fast neutral atoms which enter the detector and provides energy analysis. It is designed so that all ions produced in the 21-cm-long interaction region which pass through the detector collimator apertures are focused onto the electron multiplier. This feature was verified by monitoring the electron multiplier first dynode current and comparing this current with the current measured by the Faraday cup when it was moved in front of the beam. This comparison was made both using the auxiliary source as an ion source and by measuring directly ions produced by stripping of K on O_2 gas atoms. The outer cylinder of the cylindrical analyzer has an opening machined in it to permit neutrals entering the analyzer to escape without striking analyzer surfaces. The opening is covered with a nickel grid having an optical transmission of 98%.

The surface ionization detector consists of a 0. 0127-mm-thick tantalum ribbon preceded by a 90% transmission nickel grid for ion collection. The grid is placed 1. 25 mm in front of the ribbon. [3]

III. EXPERIMENTAL PROCEDURE

In order to measure the cross section for ionization of K on impact with gas target molecules under single-collision conditions, it is necessary to measure a number of quantities. In particular, this cross section is given by

$$I_+ = I_0 \sigma_{01} \rho l , \qquad (2)$$

where I_+ is the total number of K ions produced by ionization, I_0 is the incident fast atom flux, ρ is the target gas density, l is the length of the collision region, and σ_{01} is the required cross section. For our experiment, l was 21 cm.

The density ρ is calculated from the target gas pressure measured with a glass enclosed Bayard-Alpert gauge. The manufacturer's experience with gauges that have been compared with absolute standards is that generally the "off-the-shelf" gauge reads within 20% of the absolute value. [19] Since our

gauge was not compared with an absolute standard, consistency checks were made to ensure that it was not atypical. First, it was compared with two other Bayard-Alpert gauges of the same manufacture also installed in the collision chamber. One of these was an identical glass enclosed gauge, the other was of nude design. The outputs of the three gauges agreed to within 10%.

Second, the following procedure served as a check on the relative pressure measurements of the four target gases. The target gas entered the collision chamber through a collimated hole structure. This in effect constituted a porous plug which restricted the gas flow into the chamber. Thus, when the ion gauge read 1×10^{-5} Torr for N_2, the pressure behind the collimated hole structure, measured with a capacitance manometer, was 10 Torr. Alternatively, for gases other than N_2 for a capacitance manometer reading of 10 Torr, the corresponding collision chamber pressure was 1×10^{-5} Torr when the ion gauge reading was corrected for the ionization probability of the test gas relative to that of N_2. During measurements of ionization produced, the target gas pressure was maintained at 1×10^{-5} Torr. This is sufficiently low to ensure that single-particle collision conditions prevail.

It thus remains to measure the quantities I_+ and I_0 using the detectors described in Sec. II and schematically shown in Fig. 1. I_0 was measured absolutely using surface ionization detection techniques developed specifically for fast atoms. These are discussed in detail elsewhere. [2,3] I_+ was measured with the cylindrical analyzer detector. The auxiliary ion source was used initially to calibrate both the cylindrical analyzer and its associated electron multiplier and also to verify independence of the multiplier gain as a function of background gas. The auxiliary ion source was operated with a positive voltage equal to the desired energy as the bias on the emitter. The outer apertures of the einsel lens were at ground potential, and the center one was adjusted to focus the beam.

To calibrate the cylindrical analyzer, the cylinder potentials were adjusted with a positive voltage on the outer cylinder and an equal negative voltage on the inner one in the presence of the incident auxiliary ion beam until the signal output of the electron multiplier was a maximum. The optimum voltage difference V between the analyzer cylinders thus determined for optimum focus for a given ion energy E was $V = 0.4E$. This calibration was established for ion energies in the range 5 to 1000 eV, although for the present experiments no thresholds below about 10 eV occur and the sensitivity of our detectors is such that it limits measurement to cross sections of about 10^{-20} cm^2 or greater. Electrometers connected to the cylinders confirmed that

all the ions entering the analyzer were entering the electron multiplier when its signal output was a maximum.

The sensitivity $\Delta V/V$ of the cylindrical analyzer is about 0.025 where $\pm \Delta V$ is the deviation from V for which no loss in signal from the analyzer occurs. Within the limits of this sensitivity, the setting V required for optimum focus of a given energy ion from the auxiliary source was identical to that of a collisionally ionized fast atom where an energy loss of 4.3 eV from the fast-beam energy is assumed. Both the fast atom and the auxiliary ion energies were monitored with a digital voltmeter having an accuracy of 0.1% by measuring the bias on the zeolite source and the charge-transfer cylinder, respectively.

Next, using the cylindrical analyzer calibration, the gain of its electron multiplier was determined as a function of energy. This was done by measuring the ion current from the auxiliary source, first, directly with the Faraday cup and then with the cylindrical analyzer aligned along the beam axis. Calibration checks were made several times during all experiments to ensure that the electron-multiplier gain remained constant. This proved to be the case for all gases used except N_2 which appeared to cause marked deterioration of the electron multiplier during the course of a data run. Thus, for N_2 it was necessary to recalibrate the electron multiplier several times during an experiment.

Upon determination of the tube gain, the auxiliary ion source was moved aside and the fast-K-atom beam was directed into the collision chamber. The fast-beam profile was measured by sweeping the surface ionization detector slowly across the beam at a constant rate and monitoring its collector current with an electrometer whose output fed into a strip chart recorder.

Next, the same procedure was repeated with the cylindrical analyzer with the collision chamber backfilled to 1×10^{-5} Torr of the target gas. This resulted in the distribution of K ions produced.

The cross section for ionization of K on impact with O_2 proved large enough that it was possible to measure I_+ directly with the Faraday cup for energies in excess of 100 eV. This agreed to within 5% with the I^+ as measured by the cylindrical analyzer. In measurements with gases other than O_2, the electron-multiplier gain was not established using the Faraday cup and auxiliary source technique. Rather it proved more convenient to measure I_+ with oxygen in the chamber, and thus infer the gain from the previously determined potassium ionization cross section on O_2. Thus, the other reported cross sections are all referenced to O_2.

It was noted by Bydin and Bukhteev[14] that in the ionization cross sections for the systems they studied, all the charged particles were forward scattered. The present data agree with their observation. In the present experiment, the profiles of the incident neutral beam and resultant charged beam are proportional, i.e., the ratio of the peak amplitudes of the two is always the same as the corresponding ratio of the integrated areas under the beam profiles. Thus, since the shapes of the two beam profiles were the same, the ratio of the peak amplitudes was sufficient to determine total ionization cross sections reported here.

IV. RESULTS

Figure 3 shows the results for ionization of K on H_2, CO, N_2, and O_2. The cross sections are plotted against fast K-atom velocity in the laboratory system, on a log-log scale. Table I is a tabulation
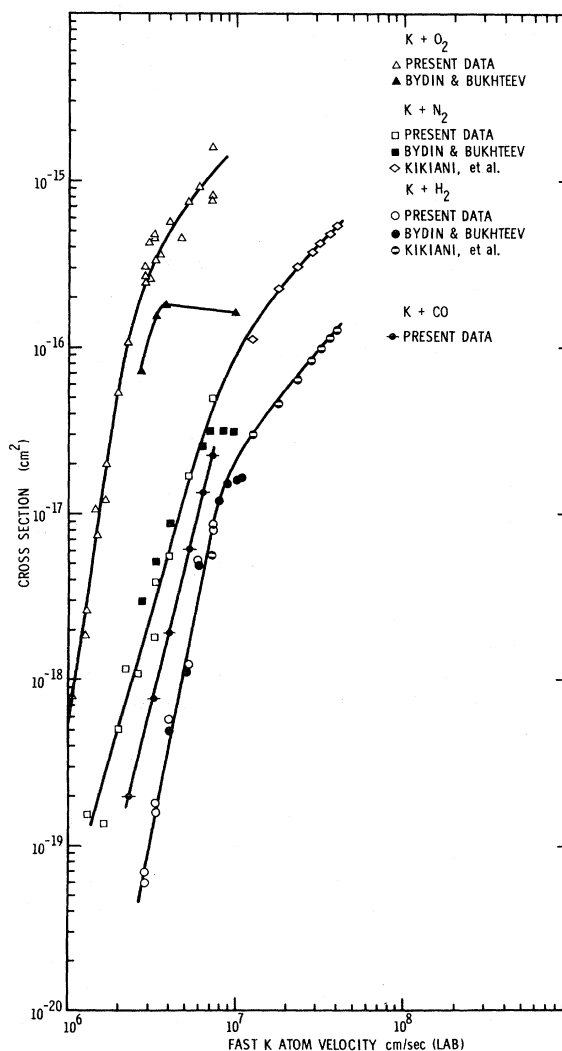
FIG. 3. Cross sections for ionization of potassium on impact with H_2, N_2, O_2, and CO as a function of potassium-atom velocity.

TABLE I. Tabulation of data.

Fast atom velocity (cm/sec)	σ_{01} (cm^2)
K + O$_2$	
1.04×10^6	8×10^{-19}
1.25×10^6	1.8×10^{-18}
1.28×10^6	2.6×10^{-18}
1.45×10^6	7.5×10^{-18}
1.45×10^6	1.05×10^{-17}
1.65×10^6	1.2×10^{-17}
1.7×10^6	2×10^{-17}
2×10^6	5.4×10^{-17}
2.25×10^6	1.05×10^{-16}
2.8×10^6	2.4×10^{-16}
2.8×10^6	2.6×10^{-16}
2.8×10^6	3×10^{-16}
3×10^6	2.6×10^{-16}
3×10^6	4.2×10^{-16}
3.2×10^6	4.5×10^{-16}
3.2×10^6	4.7×10^{-16}
3.3×10^6	3.4×10^{-16}
3.5×10^6	3.6×10^{-16}
4×10^6	5.6×10^{-16}
5.2×10^6	7.5×10^{-16}
6.1×10^6	9.1×10^{-16}
7.2×10^6	1.6×10^{-15}
7.2×10^6	8×10^{-16}
7.2×10^6	7.5×10^{-16}
K + N$_2$	
1.3×10^6	1.55×10^{-19}
1.65×10^6	1.35×10^{-19}
2×10^6	5×10^{-19}
2.2×10^6	1.15×10^{-18}
2.6×10^6	1.1×10^{-18}
3.3×10^6	1.8×10^{-18}
3.3×10^6	3.9×10^{-18}
4×10^6	5.5×10^{-18}
5.2×10^6	1.7×10^{-17}
7.2×10^6	5×10^{-17}
K + CO	
2.3×10^6	2×10^{-19}
3.3×10^6	7.7×10^{-19}
4×10^6	1.9×10^{-18}
5.2×10^6	6.1×10^{-18}
6.4×10^6	1.35×10^{-17}
7.2×10^6	2.25×10^{-17}
K + H$_2$	
2.85×10^6	5.9×10^{-20}
2.8×10^6	6.8×10^{-20}
3.3×10^6	1.6×10^{-19}
3.35×10^6	1.8×10^{-19}
4×10^6	5.8×10^{-19}
5.2×10^6	1.25×10^{-18}
6×10^6	5.3×10^{-18}
7.2×10^6	5.6×10^{-18}
7.3×10^6	8×10^{-18}
7.3×10^6	8.8×10^{-18}

of the data. Presented also, in Fig. 3, for comparison, are the data of Kikiani et al.[15] for the systems K-H$_2$ and K-N$_2$, and those of Bydin and Bukhteev for the systems K-H$_2$, K-N$_2$, and K-O$_2$. The present data for oxygen lies somewhat higher than those of Bydin and Bukhteev,[14] and their curves for N$_2$, O$_2$, and H$_2$ bend over more sharply. However, in two cases the present data can be reasonably extrapolated to that of Kikiani et al.[15]

For the species investigated here, the near-threshold behavior can be described satisfactorily by the empirical relationship

$$\sigma_{01} = \sigma_0 [(v/v_0)^m - 1] . \tag{3}$$

In Eq. (3) σ_0 is the value of the cross section at the theoretical threshold velocity v_0, if one linearly extrapolates the "near-threshold" cross section on the log-log plot. The exponent m is the slope of the experimentally measured cross-section curve, near threshold, as obtained from Fig. 3.

Table II summarizes the parameters σ_0 and m of Eq. (3) as obtained from the data of Fig. 3 and in addition the theoretical threshold velocity v_0 and energy E_0, obtained from Eq. (1).

The experimental uncertainty in the cross-section data presented here is estimated as follows: The beam path l was measured to within 5%. Because the Bayard-Alpert gauge used for the gas density measurement was not calibrated against an absolute standard, the 20% uncertainty indicated by the manufacturer's comparisons with absolute standards is used. The fast neutral K beam flux was measured to within 10% as reported previously.[2,3] The flux of ionized potassium atoms corresponding to cross sections in excess of about 10^{-18} cm^2 was measured to 5% accuracy or better. For smaller cross sections this uncertainty is conservatively estimated as 10%. Thus, the rms systematic uncertainty of the cross sections σ_{01} presented in this paper is about 25%. On repeated measurements, the cross sections proved to be reproducible to better than 10%.

TABLE II. Summary of theoretical thresholds for ionization of K and experimental values for the parameters of Eq. (3).

Colliding particles	E_0	v_0 (cm/sec)	m	σ_0 (cm^2)
K-O$_2$	9.55	6.9×10^5	7.0	5×10^{-20}
K-N$_2$	10.3	7.3×10^5	3.54	1.4×10^{-20}
K-CO	10.3	7.3×10^5	4.05	1.7×10^{-21}
K-H$_2$	88	2.1×10^6	5.26	1.25×10^{-20}

V. DISCUSSION

A. Experimental

The discrepancy between the present results and those of Bydin and Bukhteev is not understood. A possible explanation for the more rapid turnover in the Bydin and Bukhteev[14] data relative to the present results and those of Kikiani et al.[15] is production of secondary electrons by fast atoms at their Faraday cup collimating apertures. During development of fast-atom detectors this has been found to be as much as 20–50% of the fast-beam intensity for fast-atom energies above 150 eV.[3] The quantitative difference between the present data and those of Bydin and Bukhteev[14] in the case of O_2 is particularly strange since the present N_2 and H_2 cross sections referenced to O_2 are in general quantitative agreement with both the Bydin and Bukhteev[14] and Kikiani et al.[15] results. These kinds of differences in atomic physics experiments are often due to differing populations of excited states. This appears unlikely here. Both the present experiment and that of Bydin and Bukhteev[14] used resonant charge transfer of a thermionically derived ion beam to produce the fast neutral beam. The Kikiani et al.[15] group used nitrogen as the charge-transfer gas. Perel and Daley[20] recently showed that charge transfer occurs preferentially in the channel having the smallest energy defect, i.e., a near-resonant charge transfer appears preferred to the ground state. Thus, it is improbable that the thermally produced ions, presumably in the ground state, charge transfer to an excited state. On the basis of the work by Perel and Daley,[20] one would therefore anticipate differences between the present data and those of Kikiani et al.[15] rather than those of Bydin and Bukhteev[14] if excited-state populations were present.

B. Theoretical

Projectile-atom ionization produced in fast-atom-atom collisions is generally attributed to atomic stripping. Atomic stripping of heavy atoms is thought to proceed by way of potential-curve crossing as first described by Landau,[21] Zener,[22] and Stueckelberg.[23] However, the potential curves for heavy atoms are not known even approximately, so direct calculation is precluded. Thus, the several attempts to devise theories for atomic stripping are all statistical theories.[24–26] Of these efforts, the theory of Firsov appears to be the most successful if only because it alone gives a definite prediction without adjustable parameters.

Comparing the present experimental results to Firsov's predictions leads to the conclusion that the theory is not applicable in the low-energy regime. In particular the Firsov scaling law is too weak to account for the 10^3 range in cross section for targets of atomic numbers ranging from $Z = 1$ to $Z = 16$. Even for higher energies the general Firsov scaling law at best seems to suggest only what the upper bound of a given cross section might be. The distribution of experimentally measured cross sections varies over several orders of magnitude below it. Fleischmann and Dehmel[27] have recently proposed a semiempirical scaling relationship which significantly compresses the normalized distribution of high energy observations relative to the Firsov scaling law. However, in the low-energy regime it suffers from the same deficiency.

It must, however, be noted that stripping is not the only reaction which can account for the measured ionization cross sections. Compton et al.[12] recently measured relative cross sections for the reaction $Cs + O_2 \rightarrow Cs^+ + O_2^-$. It appears probable that like reactions occur for impact of potassium on diatomic species as well in which case the statistical theory may not be applicable.

ACKNOWLEDGMENTS

†Work was supported by the U. S. AEC.

[1]J. Politiek and J. Los, Rev. Sci. Instr. 40, 1576 (1969).

[2]J. F. Cuderman, Rev. Sci. Instr. 42, 583 (1971).

[3]J. F. Cuderman, Surface Sci. 28, 569 (1972).

[4]N. G. Utterback and G. H. Miller, Phys. Rev. 124, 1477 (1961).

[5]N. G. Utterback, J. Chem. Phys. 44, 2540 (1966).

[6]R. C. Amme and P. O. Haugsjaa, Phys. Rev. 177, 230 (1969).

[7]H. C. Hayden and N. G. Utterback, Phys. Rev. 135, 1575A (1964).

[8]H. C. Hayden and R. C. Amme, Phys. Rev. 141, 30 (1966).

[9]N. G. Utterback and Bert Van Zyl, Phys. Rev. Letters 20, 1021 (1968).

[10]H. H. Fleischmann and R. A. Young, Phys. Rev. 178, 254 (1969).

[11]H. H. Fleischman and R. A. Young, Phys. Letters 29A, 287 (1969).

[12]R. N. Compton, S. J. Nalley, H. C. Schweinler, and V. E. Anderson, in Proceedings Seventh International Conference on the Physics of Electronic and Atomic Collisions (North-Holland, Amsterdam, 1971), Vol. I, p. 228.

[13]G. Gerber, R. Morgenstern, A. Niehaus, and M. W.

Ruf, in Ref. 12, p. 610.

[14]Y. F. Bydin and A. M. Bukhteev, Zh. Tech. Fiz. 30, 546 (1960) [Sov. Phys. Tech. Phys. 5, 512 (1960)].

[15]B. I. Kikiani, G. N. Ogurtsov, N. V. Federenko, and I. P. Flaks, Zh. Eksperim. i Teor. Fiz. 49, 379 (1965) [Sov. Phys. JETP 22, 264 (1966)].

[16]R. E. Weber and L. F. Cordes, Rev. Sci. Instr. 37, 112 (1966).

[17]J. C. King and J. R. Zacharias, Advan. Electron. Electron Phys. 8, (1956).

[18]J. F. Cuderman, Rev. Sci. Instr. 42, 1094 (1971).

[19]W. Wheeler, Research and Development Group, Vacuum Products Division, Varian and Associates, private commumication.

[20]J. Perel and H. Daley, in Ref. 12, p. 603.

[21]L. D. Landau, Phys. Sowjetunion 2, 46 (1932).

[22]C. Zener, Proc. Roy. Soc. (London) A137, 696 (1932).

[23]E. C. G. Stueckelberg, Helv. Phys. Acta 5, 370 (1932).

[24]A. Russek, Phys. Rev. 132, 246 (1963).

[25]M. H. Mittleman and L. Wilets, Phys. Rev. 154, 12 (1967).

[26]O. B. Firsov, Zh. Eksperim. i Teor. Fiz. 36, 1517 (1959) [Sov. Phys. JETP 36, 1076 (1959)].

[27]H. Fleischmann and R. Dehmel, in Ref. 12, Vol. II, p. 1146.

Formation of Fast Excited H Atoms. I. Charge-Transfer Neutralization of H⁺ in He and Ar[†]

J. C. Ford and E. W. Thomas*

School of Physics, Georgia Institute of Technology, Atlanta, Georgia 30332

(Received 17 September 1971)

A study has been made of the charge-transfer processes whereby neutral atoms of hydrogen are formed in the $3s$, $3p$, and $3d$ states as a result of the impact of protons on targets of helium and argon. Impact energies range from 75 to 400 keV. The experimental procedures involve the quantitative measurement of the Balmer-α radiation emitted by the spontaneous decay of atoms in these three states. The contributions of the three different states are separated by a time-of-flight technique that utilizes the different lifetimes of these states. The cross sections decrease rapidly with increasing energy and are greatest for the state of lowest angular-momentum quantum number. For a helium target, comparisons are made with a Born-approximation prediction; there is a marked discrepancy between theory and experiment for the $3p$ level but good agreement for the $3s$ and $3d$ levels.

I. INTRODUCTION

The objective of the present study is the measurement of cross sections for formation of fast excited hydrogen atoms in the $3s$, $3p$, and $3d$ states by the impact of protons on helium and argon targets. The reaction may be described by

$$H^+ + X \to H^* \ (3s, \ 3p, \ \text{or} \ 3d) + [X^+], \tag{1}$$
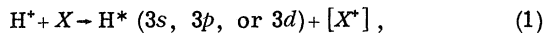
where X is either helium or argon. The square bracket in Eq. (1) indicates that there is no information on the post-collisional state of the target. The principal objective of the work was to test the theoretical predictions of charge-transfer cross sections. It has previously been argued[1] that formation of the $n = 3$ levels by neutralization of H^+ is a particularly useful case for making such tests.

II. EXPERIMENTAL TECHNIQUES

The formation of excited H atoms in the $3s$, $3p$, and $3d$ states can be detected by the quantitative measurement of Balmer-α photons emitted as excited atoms decay to the $n = 2$ level. The Balmer-α (H_α) emission is, in fact, due to three transitions:

$3s \to 2p$, $3p \to 2s$, and $3d \to 2p$. These will emit photons of essentially the same wavelength and are therefore detected simultaneously. The separation of the three contributions is accomplished by a method which relies on the different lifetimes of the three states.

The experimental arrangement involves passing the beam through a target cell and measuring quantitatively the Balmer-α emission from the beam after it exits into an evacuated flight tube. Excited fast atoms, formed by neutralization in the target cell, decay in the observation region and produce an intensity whose spatial variation is related to the velocity of the atom and the lifetime of the excited state. The radiation may be described by an intensity function $I(X)$, where X is the distance from the termination of the gas cell. The function $I(X)$ is defined as the total number of Balmer-α photons radiated per second from a differential segment of beam dX about the point X. Since each state of excitation ($3s$, $3p$, and $3d$) has a distinctly different lifetime, the total intensity function $I(X)$ will be the sum of three spatially distinct and separable intensity functions, $I_{3s}(X)$, $I_{3p}(X)$, and $I_{3d}(X)$. The intensity $I_{3l}(X)$ is given by